



RESEARCH LETTER

10.1029/2023GL103944

How Important Are Horizontal Eddy Moisture Transports for the MJO's Eastward Propagation?

S. N. Tulich^{1,2} ¹CIRES, University of Colorado Boulder, Boulder, CO, USA, ²NOAA Physical Sciences Laboratory, Boulder, CO, USA

Key Points:

- A novel approach for assessing the role of horizontal eddy moisture transports in fostering the Madden-Julian oscillation (MJO)'s eastward propagation is explored
- Results show that the eddy transports are generally of greater importance than those due to the MJO's own circulation anomalies
- The inclusion of spectral signals with periods greater than 20 days is essential for capturing the full effects of the eddies

Supporting Information:

Supporting Information may be found in the online version of this article.

Correspondence to:

S. N. Tulich,
stefan.tulich@noaa.gov

Citation:

Tulich, S. N. (2023). How important are horizontal eddy moisture transports for the MJO's eastward propagation? *Geophysical Research Letters*, 50, e2023GL103944. <https://doi.org/10.1029/2023GL103944>

Received 17 APR 2023

Accepted 15 JUN 2023

Abstract The eastward propagation of the Madden-Julian oscillation (MJO) is known to hinge crucially on the effects of horizontal moisture advection, which involve two main types of circulation anomalies. The first are those of the MJO itself, while the second are those of embedded Rossby-type “eddies,” which tend to be most active to the west of the MJO's convective center. To quantify the relative importance of the eddies, a novel approach is taken in which their formal definition is given by the residual of a least-squares fit to an observed bivariate MJO index. Results show that the eddies, when defined in this way, are generally of leading importance for fostering the MJO's eastward propagation in terms of column-integrated moisture. The picture is seen to be reversed, however, when using a traditional filter-based method to define the eddies, which are then strictly “high-frequency” in nature.

Plain Language Summary The Madden-Julian oscillation (MJO) is an important type of large-scale weather pattern that moves slowly eastward over the tropical Indo-Pacific for reasons that have yet to be fully explained. In particular, while the effects of winds carrying moisture are known to be essential, a question that remains open concerns the role of winds directly tied to the MJO versus those of distinct swirling “eddy” motions. A novel technique is devised for addressing this issue, which shows that the eddy motions are of leading importance over the Maritime Continent and further east, while MJO winds are of leading importance over the tropical Indian Ocean. The key eddy motions in this regard have time scales comparable to the MJO, rather than being smaller as typically conceived.

1. Introduction

The Madden-Julian oscillation (MJO) is a well-known mode of tropical intraseasonal variability that has yet to be fully explained from a mechanistic standpoint, despite decades of research. Based on numerous observational and model diagnostic efforts (see Ren et al., 2021, and the references therein) there is now little doubt that the process of horizontal moisture advection (denoted “hAdv”) is of central importance to the phenomenon, particularly as it relates to the slow eastward propagation of convection anomalies over the Indo-Pacific warm pool region. What remains unsettled however, is the extent to which the accompanying eastward-moving signals in hAdv are shaped by the MJO's own planetary-scale circulation anomalies, versus those of embedded Rossby-type “eddies” that tend to be more active (and hence more effective at transporting moisture away from the tropics) during the low-level westerly phase of the disturbance, as compared to its low-level easterly phase (Maloney & Dickinson, 2003; L. Wang et al., 2019). Indeed, while several studies have reported the eddies to be of generally leading importance (Andersen & Kuang, 2012; Benedict et al., 2015; Kiranmayi & Maloney, 2011; Maloney, 2009), others have reported their role to be mainly secondary (Berrington et al., 2022; Jiang, 2017; D. Kim et al., 2014; Wolding et al., 2016). In simple models of the MJO under the name “moisture mode,” varying levels of importance have thus been assigned to the eddies, ranging from critical (Adames & Kim, 2016), to negligible (S. Wang & Sobel, 2022), or somewhere in between (Ahmed, 2021; Sobel & Maloney, 2013).

This lack of agreement might come as surprise, given that all of the diagnostic studies just mentioned rely on essentially the same formal definition of the eddies as being the residual with respect to a lowpass filter in time. However, a distinguishing factor that seems to have gone unnoticed is whether the choice of filter cutoff is closer to a period of either 20 or 30 days. Reasons for expecting this level of difference to actually matter include the well-known tendency of lower frequencies in the tropics to contain generally more energy than higher frequencies, exclusive of the MJO (Gehne & Kleeman, 2012; Hayashi, 1974; Hendon & Wheeler, 2008). While this generic tendency would seem to argue in favor of adopting a cutoff closer to 30 days, the obvious concern is the greater potential for including the effects of MJO variability that is somewhat higher in frequency than what is

© 2023 The Authors.

This is an open access article under the terms of the [Creative Commons Attribution-NonCommercial License](https://creativecommons.org/licenses/by-nc/4.0/), which permits use, distribution and reproduction in any medium, provided the original work is properly cited and is not used for commercial purposes.

typically observed, due to the episodic nature of the phenomenon. The need to weigh this concern is unavoidable when using a lowpass filter to define the eddies.

Here, an alternative approach for calculating the eddy contribution to $hAdv$ is explored, in which the eddies are defined as the residual of a least-squares fit to an observed MJO index time series. The benefit is that the only filtering decisions needed are those used to derive the index. The next section describes the data and methods, which is then followed by an overview of results in Section 3. The main findings are summarized and discussed in Section 4.

2. Data and Methods

Two types of data are leveraged in this study. The first are satellite estimates of daily outgoing longwave radiation (OLR), which are made available by the National Oceanic and Atmospheric Administration (NOAA) at $2.5^\circ \times 2.5^\circ$ grid spacing, as described in (Liebmann & Smith, 1996). The second are three-hourly pressure-level estimates of horizontal winds and specific humidity at $0.25^\circ \times 0.25^\circ$ grid spacing, obtained from the European Centre for Medium Range Weather Forecasting (ECMWF) Reanalysis v5 (ERA5) product (Hersbach et al., 2020). To simplify the analysis, the ERA5 data were course grained to have the same spatial and temporal resolution as the NOAA OLR data. The time period of interest spans the 30-year stretch from 1990 to 2019.

In addition to the above gridded forms of data, the approach assumes an MJO index of the form: $X(t) = [X_1(t), X_2(t)]$, where X_1 and X_2 are the principal component (PC) time series of a distinct pair of empirical orthogonal functions (EOFs) that serve to delineate the MJO's evolution in terms of some judiciously chosen field (or combination of fields). The specific index adopted here is the so-called OLR-based MJO index (OMI) of Kiladis et al. (2014), which is designed to isolate the MJO's evolution in terms of convection (as opposed to zonal wind), using filtered OLR as a proxy. In addition to relying solely on OLR, a unique aspect of the OMI is that its PCs and associated EOFs are calculated separately for each calendar day, using a 120-day sliding window, to account for the MJO's known dependence on the seasonal cycle (Zhang & Dong, 2004).

Because the PCs are linearly independent from one another, they can be used to partition any dependent variable $Y(t)$ into the sum of a least-squared fitted term and its “eddy residual,” that is,

$$Y = Y_f + Y_e, \quad (1)$$

where

$$Y_f \equiv a_1 X_1 + a_2 X_2 + Y_0. \quad (2)$$

Here the quantities a_1 , a_2 , and Y_0 are the fitting parameters, which are calculated separately for each calendar day, using the same 120-day sliding window as used to derive the OMI. The eddies are thus defined as perturbations about the daily varying climatology of Y (as embodied by the intercept parameter Y_0), in addition to its linear MJO component (as embodied by the sum of $a_1 X_1$ and $a_2 X_2$, denoted Y_m). Given this definition, the horizontal advection of moisture can then be partitioned as:

$$hAdv \equiv -\mathbf{v} \cdot \nabla q = hAdv_m + hAdv_e, \quad (3)$$

where \mathbf{v} is the horizontal wind, q is specific humidity, and

$$hAdv_m \equiv -\mathbf{v}_f \cdot \nabla q_f; \quad (4a)$$

$$hAdv_e \equiv -\mathbf{v}_f \cdot \nabla q_e - \mathbf{v}_e \cdot \nabla q_f - \mathbf{v}_e \cdot \nabla q_e. \quad (4b)$$

The distinction here is thus between two types of terms, one involving only fitted quantities ($hAdv_m$; referred to as the “MJO component”) and the other involving eddy fluctuations in \mathbf{v} and/or q ($hAdv_e$; referred to as the “eddy-residual component”).

The above partitioning is quite different from that of previous studies, which have instead invariably made use of Fourier decomposition methods to write:

$$Y = \langle Y \rangle + Y', \quad (5)$$

where angle brackets denote application of a low-pass frequency filter with a cutoff at a period of either 20 or 30 days (depending on the study), and the prime denotes the resulting high-frequency residual. Here, the cutoff period is 20 days, unless otherwise stated. The analogs of the quantities $hAdv_m$ and $hAdv_e$ can then be defined respectively as:

$$hAdv_s \equiv -\langle \mathbf{v} \rangle \cdot \nabla \langle q \rangle; \quad (6a)$$

$$hAdv_h \equiv -\langle \mathbf{v} \rangle \cdot \nabla q' - \mathbf{v}' \cdot \nabla \langle q \rangle - \mathbf{v}' \cdot \nabla q', \quad (6b)$$

where the former is referred to following Chikira (2014) as the “slowly varying component,” while the latter is referred to as the “high-frequency eddy component.” While this sort of separation is by now standard, problems will generally arise in the case of “non-MJO” eddies whose signals extend across the filter cutoff, thereby precluding the basis of the separation.

The primary objective of this study is to shed light on how choices made in the partitioning of $hAdv$ affect conclusions about the role of eddies in fostering the MJO's slow eastward propagation in terms of column-integrated moisture. To this end, an MJO compositing method is devised that essentially builds on the least-squared fitting procedure already introduced. The idea is to take the additional step of linearly regressing each of the PC components, X_1 and X_2 , onto the sine and cosine of their associated phase angle θ , to obtain expressions of the form:

$$X_1^* \equiv b_1 \sin \theta + b_2 \cos \theta; \quad (7a)$$

$$X_2^* \equiv c_1 \sin \theta + c_2 \cos \theta, \quad (7b)$$

where the regression coefficients are once again calculated separately for each calendar day. Substituting these expressions for X_1 and X_2 in Equation 2, the composite phase dependence of any variable can then be calculated as:

$$Y^* = (a_1 b_1 + a_2 c_1) \sin \theta + (a_1 b_2 + a_2 c_2) \cos \theta. \quad (8)$$

Here, this expression is evaluated at a series of evenly spaced values of θ in the range $0-2\pi$, which are indexed using real numbers in the range 1–8, following standard practice.

With the above compositing procedure in hand, the following metric is then adopted:

$$S_p(hAdv_n) \equiv \frac{\| [hAdv_n]^* [\partial q_v / \partial t]^* \|}{\| [\partial q_v / \partial t]^* [\partial q_v / \partial t]^* \|}, \quad (9)$$

where the subscript “n” denotes an arbitrary partitioned component of $hAdv$, $[\cdot]$ denotes vertical integration in pressure coordinates, and $\|\cdot\|$ denotes averaging over MJO phase, calendar day, and some spatial domain of interest (described in the next section). This metric was first introduced by Andersen and Kuang (2012), who regarded it as conveying the net contribution by a given moisture source to the MJO's eastward propagation in terms of $[q_v]$. Here the physical interpretation is the same, but where it is acknowledged that this conceptualization is only strictly valid in the context of traveling plane wave disturbances.

3. Results

Before considering the partitioned components of $[hAdv]$, it is helpful to first contrast the spectral properties of the MJO versus eddy-residual parts of the flow, as viewed in terms of the divergence δ and vorticity ζ of the horizontal wind. The upper three panels in Figure 1 depict the climatological space-time spectra of δ , δ_m , and δ_e at 700 hPa across the tropical Indo-Pacific region ($60^\circ\text{E}-180^\circ\text{E}$; $15^\circ\text{S}-15^\circ\text{N}$). The bottom three panels are similar but for ζ , ζ_m , and ζ_e . The methods used to obtain these regional spectra are the same as described in Tulich and Kiladis (2021, see their Figure 1). Although such methods likely lead to some distortion of the spectra at the lowest zonal wavenumbers, due to the use of a zonal tapering window (Cheng et al., 2022), results are found to remain qualitatively unchanged when considering the global space-time spectra of vorticity and divergence (not shown).

The overall success of the fitting procedure in isolating the signals of the MJO is readily apparent in both sets of spectra in Figure 1. In the case of the divergence spectra, these signals are seen in Figure 1b to be devoid of any indication of moist Kelvin waves, the latter of whose signals are fully contained in the eddy-residual spectrum of Figure 1c, together with the familiar “red-noise” background. This separation is lost in the total divergence

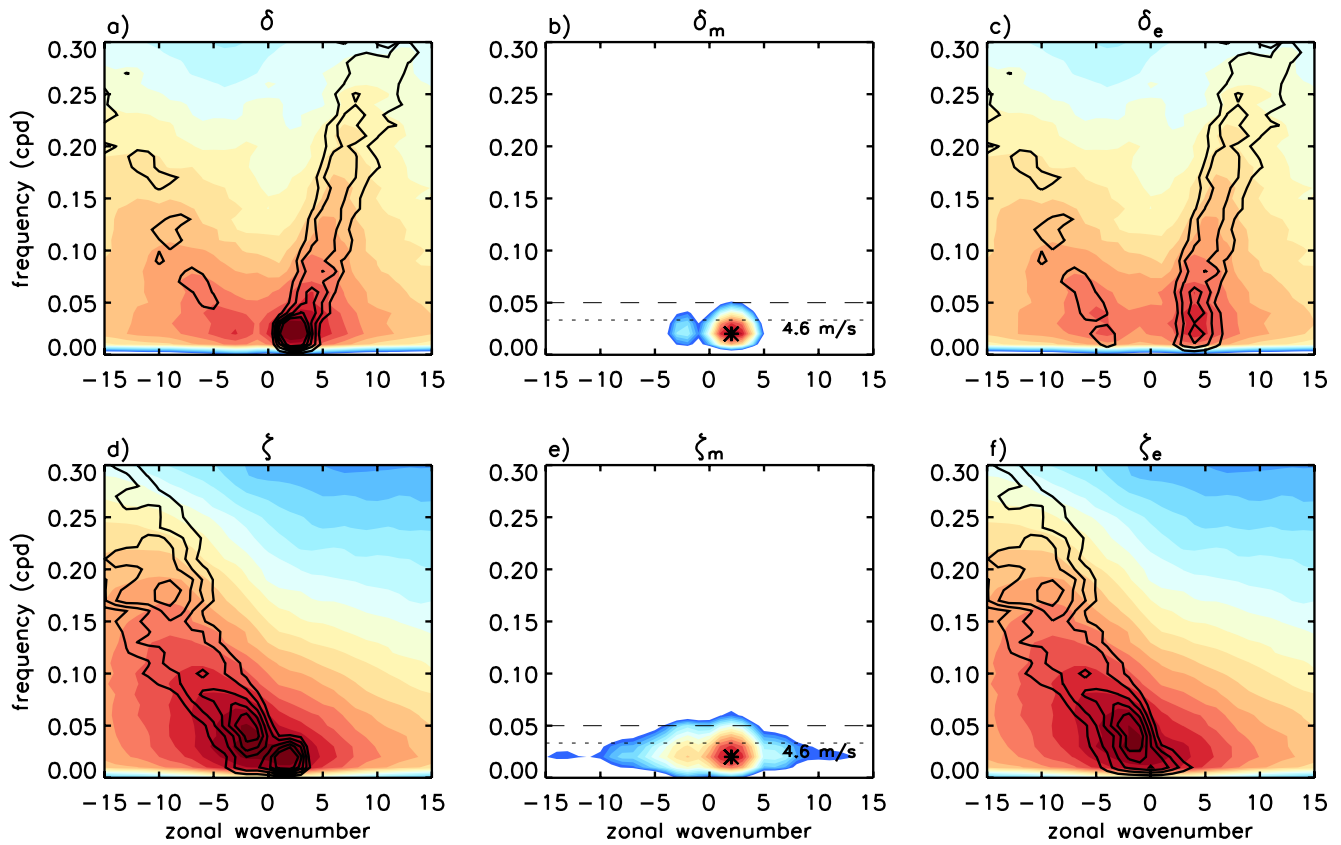


Figure 1. Climatological space-time spectra of the divergence δ and vorticity ζ of the horizontal wind at 700 hPa over the tropical Indo-Pacific sector (60°E – 180°E ; 15°S – 15°N ; upper and lower left panels, respectively), together with their Madden-Julian oscillation (MJO) (middle column) and eddy-residual (right column) components. Shading denotes the logarithm of the raw power, while contours in the left and right columns indicate where the signal-to-noise ratio exceeds 1.1, with intervals of 0.1. Symbols with annotation in the middle panels denote the location and associated phase speed of the MJO's spectral peak in the corresponding field; the dashed and dotted lines denote wave periods of 20 and 30 days, respectively.

spectrum of Figure 1a, however, where the signals of the two wave types appear to merge seamlessly with one another at zonal wavenumbers $k = 3$ and 4, apparently due to effects of tropical-extratropical interactions (Tulich & Kiladis, 2021). Regardless and perhaps of greater relevance to this study, the overall redness of the eddy-residual spectrum implies fluctuations in divergence that are more local, as opposed to wave-like, in physical space (Ricciardulli & Sardeshmukh, 2002; Yano et al., 2004).

The same is also true in the case of vorticity, but where the eddy-residual spectrum in Figure 1f is dominated by a broad lobe of enhanced westward-moving power, encompassing the signals of lower-frequency equatorial Rossby-type (ER) waves (M. Wheeler & Kiladis, 1999) to higher-frequency tropical depression-type (TD) disturbances (Takayabu & Nitta, 1993). As noted in the introduction, such swirling eddy disturbances tend to be more active during the low-level westerly phase of the MJO, as compared to its low-level easterly phase, a tendency that is of interest here in terms of its effects on [hAdv].

This tendency is readily apparent in Figure 2a, which depicts the all-season composite phase evolution of the MJO in terms of zonal wind u (contours) and the square of the eddy-residual vorticity ζ_e^2 (shading) at 700 hPa, averaged between 15°S and 15°N . Rather than being perfectly in phase with one another, however, fluctuations in ζ_e^2 are seen to slightly lead those in u , especially over the Indian Ocean (IO; 50°E – 100°E) sector, where the phase difference is around an eighth of a wave cycle. Presumably, the reason for this phase difference is tied to the effects of diabatic processes, which are known to importantly contribute to the MJO's modulation of the eddies, in addition to “dry” dynamics (Maloney & Dickinson, 2003; L. Wang et al., 2019). Evidence to support this idea is contained in Figure 2b, which shows that MJO convection anomalies (using OLR as a proxy) are largest over the IO sector, precisely where MJO zonal wind anomalies are weakest. The implication is that the MJO's modulation of the eddies transitions from being more thermally to mechanically driven, as the disturbance's convective

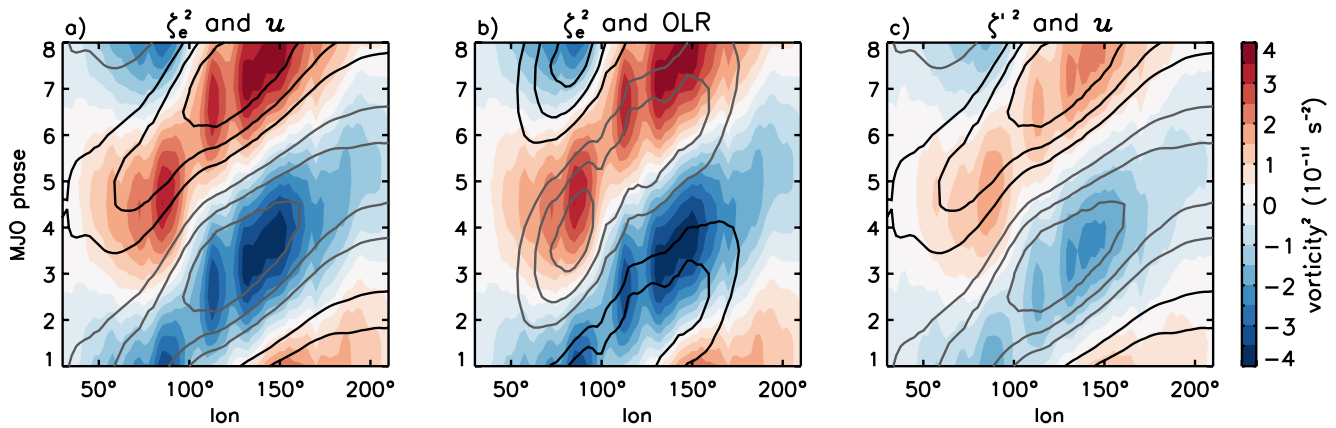


Figure 2. (a) All-season composite evolution of the Madden-Julian oscillation (MJO) at 700 hPa in terms of zonal wind u (contours) and the square of the eddy-residual vorticity ζ_e^2 (shading), averaged between 15°S and 15°N. (b) Similar to (a), but where contours denote observed OLR anomalies. (c) Similar to (a), but where shading denotes the square of the high-frequency eddy vorticity ζ'^2 . Black [gray] contours in each panel denote positive [negative] anomalies, with intervals of 0.25 m s⁻¹ for wind and 4 W m⁻² for OLR.

envelope moves eastward through the Maritime Continent (MC; 100°E–150°E) sector, before finally arriving in the Western Pacific (WP; 150°E–200°E) sector.

The story is much the same when considering the MJO's modulation of just the high-frequency eddy activity ζ'^2 . However, the amplitude of anomalies is generally smaller by around a factor of two (compare Figures 2a and 2c). While this difference is perhaps not surprising, given the overall redness of the eddy-residual vorticity spectrum in Figure 1f, it nevertheless confirms that the swirling eddy disturbances modulated by the MJO are more than just high-frequency in character. Well-studied examples of such disturbances include “westerly wind bursts” (WWBs) and their associated flanking cyclonic gyres, whose transient nature gives rise to signals that are broad in spectral space (Kiladis et al., 1994; Yano et al., 2004) and whose occurrence frequency is known to be higher during periods of low-level MJO westerlies versus easterlies (Puy et al., 2016; Seiki & Takayabu, 2007). Results further establishing these salient properties of WWBs can be found in the Supporting Information (see Narrative S1 and Figure S1 in Supporting Information S1).

Turning to the partitioned components of [hAdv], Figure 3a is similar to the composite diagrams just described, but where the shading denotes the eddy-residual component [hAdv_e]. The evolution is broadly similar to that of the eddy activity in Figure 2, but with opposite sign. As a consequence, the phasing of anomalies with respect to those in the local tendency of column-integrated moisture [$\partial q_v/\partial t$] (denoted by contours) is less optimal for

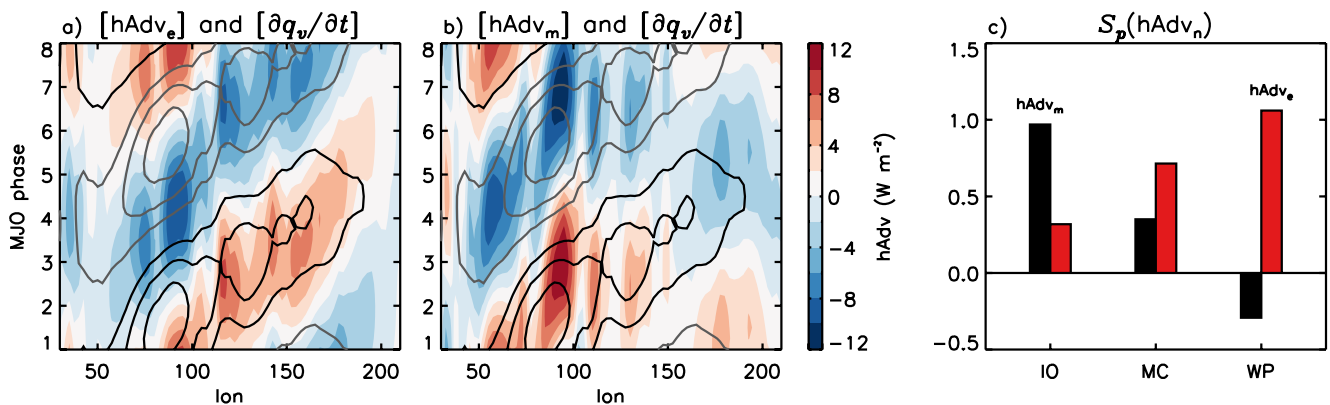


Figure 3. (a) All-season composite evolution of the Madden-Julian oscillation (MJO) in terms of the time tendency of column-integrated moisture [$\partial q_v/\partial t$] (contours with intervals of 2 W/m²; black is positive, gray is negative, and the zero contour is omitted) and the eddy-residual component of the horizontal advection of moisture [hAdv_e] (shading), averaged between 15°S and 15°N. (b) Similar to (a), but where shading denotes the MJO component [hAdv_m]. (c) Net contribution S_p by each of the two advection components [hAdv_m] (black) and [hAdv_e] (red), to the MJO's eastward propagation in terms of column-integrated moisture between 15°S and 15°N, for three different sectors of the tropical Indo-Pacific: IO (50°E–100°E), MC (100°E–150°E), and WP (150°E–200°E).

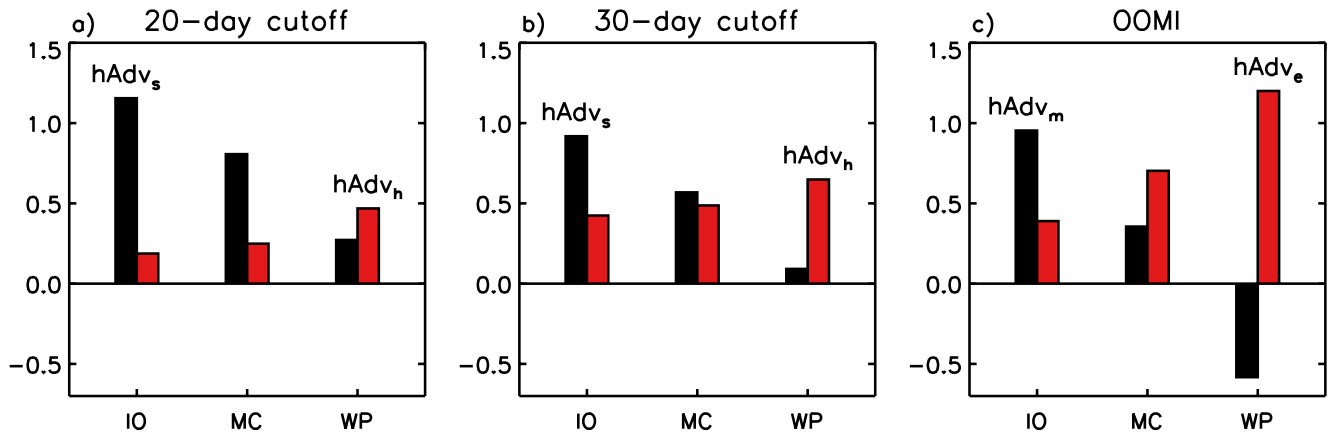


Figure 4. Similar to Figure 3c, but for: (a) the frequency-based partitioning of [hAdv] using a lowpass filter cutoff of 20 days; (b) the frequency-based partitioning of [hAdv], using a lowpass filter cutoff of 30 days; and (c) the linear regression-based partitioning of [hAdv], using the OOMI (rather than OMI) to define the state of the Madden-Julian oscillation (see text for details).

fostering the MJO's eastward propagation over the IO sector, as compared to further east. The opposite is true for the MJO component [hAdv_m], however, where anomalies are both large and more-or-less in phase with those in $[\partial q_v/\partial t]$ over the IO sector, compared to being relatively weak and out of phase over the WP sector (see Figure 3b). The amplitude and phasing of anomalies is somewhere between these two extremes over the MC sector. In accordance with previous studies (Jiang, 2017; Kiranmayi & Maloney, 2011), much of the reason for this eastward reversal in phasing of [hAdv_m] is found to be tied to the effects of MJO zonal winds blowing across zonal gradients in mean-state moisture (i.e., $u_m \partial q_0/\partial x$; see Figure S2 in Supporting Information S1). Comparing the two components in terms of the propagation metric S_p (hAdv_p), Figure 3c shows that the eddy-residual component is of leading importance for fostering the MJO's eastward propagation over both the MC and WP sectors, while the MJO component is of leading importance over the IO sector. This result holds when considering the narrower tropical belt 5°S–5°N, as well as when considering seasonal composites of the MJO (see Figures S3 and S4 in Supporting Information S1).

Figure 4a illustrates how the above picture changes when the quantity S_p is instead separated into contributions by the “slowly varying” versus “high-frequency eddy” components [hAdv_s] and [hAdv_h], respectively. The fact that the latter is of minor importance everywhere, except over the WP sector, is perhaps not surprising, given the amplitude differences in the high-frequency versus residual eddy vorticity variance shown previously in Figure 2. Rather than supporting the notion that the effects of the eddies are thus generally negligible, however, this result merely establishes the central importance of eddy fluctuations with periods greater than 20 days, which are defined in this case as “slowly varying.” Further confirmation of this point can be found in Figure 4b, which shows how the high-frequency eddy contribution becomes substantially larger upon adopting a more generous definition of “high-frequency” to include periods less than 30 days. The increase is such that the eddy contribution is on par with that of the slowly varying component over the MC region, while still remaining secondary (though of greater importance) over the IO region. An important caveat to this increased importance, however, is that at least some of it likely stems from a larger fraction of the MJO's circulation anomalies being classified as high-frequency (see Figure 4e), reflecting an inherent limitation of the approach.

The stark sensitivity to the choice of filter cutoff leads naturally to questions about whether a similar sensitivity holds in the context of the regression-based partitioning of hAdv, where such choices are necessary for constructing the MJO index used in the approach. To address this issue, an available variant of the OMI (termed “OOMI”) was used instead, where the only difference between the two indices is in terms of the filter applied to the OLR data, prior to the latter's projection onto the pair of leading EOF patterns (see Kiladis et al., 2014, for details). Specifically, the filter is revised to retain only eastward-moving zonal wavenumbers with periods in the range 30–96 days, as compared to the original choice of 20–96 days. As can be seen by comparing Figures 4c and 3c, the net effect of adopting this revision is to enhance the residual eddy contribution, similar to what was found in the case of broadening the definition of high-frequency to include periods in the range 20–30 days. The fractional degree of enhancement, however, is somewhat smaller in this case. The reason stems from the fact

that the residual-eddy component of the flow, as defined using the OMI, already includes a substantial amount of variance at periods greater than 20 days, as documented in Figure 1. While the focus of this study was on the OMI of (Kiladis et al., 2014), other indices that should be explored in the future include the modified version of the OMI described in Weidman et al. (2022), as well as the predominantly circulation-based index of M. C. Wheeler and Hendon (2004).

4. Summary and Concluding Remarks

A novel strategy was devised for quantifying the horizontal eddy advective contribution to the MJO's eastward propagation in terms of column-integrated moisture. The approach is to define the eddies as disturbances about the seasonal cycle whose evolution is linearly independent of the state of the MJO, as determined using a bivariate MJO index. Results established that the contribution by the eddies, when defined in this way, is generally of leading importance in comparison to that of the MJO's own circulation anomalies. The one exception is over the Indian Ocean basin, where the MJO's modulation of the eddies appears to stem more from fluctuations in convection, as opposed to low-level zonal wind.

To place these findings in the context of previous studies, an additional analysis was performed in which the horizontal advection of moisture $hAdv$ was separated into its more traditional “slowly varying” and “high-frequency eddy” components, using the time-honored approach of Fourier filtering. Results in this case showed a generally weaker eddy contribution, especially when adopting a definition for “high frequency” as periods less than 20 days, as compared to the more generous (though problematic) alternative of 30 days. The implication is that the eddies of leading importance have peak signals that reside toward the low-frequency end of a broad continuum of westward-moving Rossby-type variability over the tropical Indo-Pacific, rather than the high-frequency end, as typically conceived in the literature. Likely examples of such eddies include westerly wind bursts and their associated flanking cyclonic gyres, whose typical evolution was confirmed in the Supplementary Information to involve intraseasonal scales of oscillation.

In addition to bolstering our mechanistic understanding of the MJO, results of this study may also help to explain why depictions of the phenomenon are often seen to be lacking in models used to predict weather and climate, especially over the Maritime Continent region (H. Kim et al., 2019). Specifically, it is not hard to imagine how this problem might arise due to the known tendency of such models to produce artificial “grid-point” storms in the tropics, which likely come at the expense of broader eddy motions (Park & Han, 2021). Going forward, it is hoped that by investigating this issue more fully, our ability to make reliable forecasts of global weather lead times beyond 2 weeks might 1 day be improved.

Data Availability Statement

All of the regression models of $[hAdv]$ generated as part of this study are freely available for download in NetCDF format at: https://downloads.psl.noaa.gov/Projects/FAIR_paper_data/20220829_01/.

References

- Adames, Á. F., & Kim, D. (2016). The MJO as a dispersive, convectively coupled moisture wave: Theory and observations. *Journal of the Atmospheric Sciences*, 73(3), 913–941. <https://doi.org/10.1175/JAS-D-15-0170.1>
- Ahmed, F. (2021). The MJO on the equatorial Beta plane: An eastward-propagating Rossby wave induced by meridional moisture advection. *Journal of the Atmospheric Sciences*, 78(10), 3115–3135. <https://doi.org/10.1175/JAS-D-21-0071.1>
- Andersen, J. A., & Kuang, Z. (2012). Moist static energy budget of MJO-like disturbances in the atmosphere of a zonally symmetric aquaplanet. *Journal of Climate*, 25(8), 2782–2804. <https://doi.org/10.1175/JCLI-D-11-00168.1>
- Benedict, J. J., Pritchard, M. S., & Collins, W. D. (2015). Sensitivity of MJO propagation to a robust positive Indian Ocean dipole event in the superparameterized cam sensitivity of MJO propagation to a robust positive Indian Ocean dipole event in the superparameterized CAM. *Journal of Advances in Modeling Earth Systems*, 7(7), 1901–1917. <https://doi.org/10.1002/2015MS000530>
- Berrington, A. H., Sakaeda, N., Dias, J., & Kiladis, G. N. (2022). Relationships between the eastward propagation of the Madden-Julian oscillation and its circulation structure. *Journal of Geophysical Research: Atmospheres*, 127(16), e2021JD035806. <https://doi.org/10.1029/2021JD035806>
- Cheng, Y.-M., Tulich, S., Kiladis, G. N., & Dias, J. (2022). Two extratropical pathways to forcing tropical convective disturbances. *Journal of Climate*, 35(20), 6587–6609. <https://doi.org/10.1175/JCLI-D-22-0171.1>
- Chikira, M. (2014). Eastward-propagating intraseasonal oscillation represented by Chikira–Sugiyama cumulus parameterization. Part II: Understanding moisture variation under weak temperature gradient balance. *Journal of the Atmospheric Sciences*, 71(2), 615–639. <https://doi.org/10.1175/JAS-D-13-038.1>
- Gehne, M., & Kleeman, R. (2012). Spectral analysis of tropical atmospheric dynamical variables using a linear shallow-water modal decomposition. *Journal of the Atmospheric Sciences*, 69(7), 2300–2316. <https://doi.org/10.1175/JAS-D-10-05008.1>

Acknowledgments

Funding for this work was provided by the National Science Foundation (NSF) through Grant AGS-1839741. Helpful comments provided by Brandon Wolding, Adam Sobel, and two anonymous reviewers led to substantial improvements in the paper.

- Hayashi, Y. (1974). Spectral analysis of tropical disturbances appearing in a GFDL general circulation model. *Journal of the Atmospheric Sciences*, 31(1), 180–218. [https://doi.org/10.1175/1520-0469\(1974\)031<0180:SAOTDA>2.0.CO;2](https://doi.org/10.1175/1520-0469(1974)031<0180:SAOTDA>2.0.CO;2)
- Hendon, H. H., & Wheeler, M. C. (2008). Some space–time spectral analyses of tropical convection and planetary-scale waves. *Journal of the Atmospheric Sciences*, 65(9), 2936–2948. <https://doi.org/10.1175/2008jas2675.1>
- Hersbach, H., Bell, B., Berrisford, P., Hirahara, S., Horányi, A., Muñoz-Sabater, J., et al. (2020). The ERA5 global reanalysis. *Quarterly Journal of the Royal Meteorological Society*, 146(730), 1999–2049. <https://doi.org/10.1002/qj.3803>
- Jiang, X. (2017). Key processes for the eastward propagation of the Madden-Julian oscillation based on multimodel simulations. *Journal of Geophysical Research: Atmospheres*, 122(2), 755–770. <https://doi.org/10.1002/2016JD025955>
- Kiladis, G. N., Dias, J., Straub, K. H., Wheeler, M. C., Tulich, S. N., Kikuchi, K., et al. (2014). A comparison of OLR and circulation-based indices for tracking the MJO. *Monthly Weather Review*, 142(5), 1697–1715. <https://doi.org/10.1175/MWR-D-13-00301.1>
- Kiladis, G. N., Meehl, G. A., & Weickmann, K. M. (1994). Large-scale circulation associated with westerly wind bursts and deep convection over the Western equatorial Pacific. *Journal of Geophysical Research*, 99(D9), 18527–18544. <https://doi.org/10.1029/94JD01486>
- Kim, D., Kug, J.-S., & Sobel, A. H. (2014). Propagating versus nonpropagating Madden–Julian oscillation events. *Journal of Climate*, 27(1), 111–125. <https://doi.org/10.1175/JCLI-D-13-00084.1>
- Kim, H., Janiga, M. A., & Pegion, K. (2019). MJO propagation processes and mean biases in the SubX and S2S reforecasts. *Journal of Geophysical Research: Atmospheres*, 124(16), 9314–9331. <https://doi.org/10.1029/2019JD031139>
- Kiranmayi, L., & Maloney, E. D. (2011). Intraseasonal moist static energy budget in reanalysis data. *Journal of Geophysical Research*, 116(D21). <https://doi.org/10.1029/2011JD016031>
- Liebmann, B., & Smith, C. A. (1996). Description of a complete (interpolated) outgoing longwave radiation dataset. *Bulletin of the American Meteorological Society*, 77(6), 1275–1277. Retrieved from www.jstor.org/stable/26233278
- Maloney, E. D. (2009). The moist static energy budget of a composite tropical intraseasonal oscillation in a climate model. *Journal of Climate*, 22(3), 711–729. <https://doi.org/10.1175/2008JCLI2542.1>
- Maloney, E. D., & Dickinson, M. J. (2003). The intraseasonal oscillation and the energetics of summertime tropical western north Pacific synoptic-scale disturbances. *Journal of the Atmospheric Sciences*, 60(17), 2153–2168. [https://doi.org/10.1175/1520-0469\(2003\)060<2153:TIOATE>2.0.CO;2](https://doi.org/10.1175/1520-0469(2003)060<2153:TIOATE>2.0.CO;2)
- Park, S.-B., & Han, J.-Y. (2021). Suppressing grid-point storms in a numerical forecasting model. *Atmosphere*, 12(9), 1194. <https://doi.org/10.3390/atmos12091194>
- Puy, M., Vialard, J., Lengaigne, M., & Guilyardi, E. (2016). Modulation of equatorial Pacific westerly/easterly wind events by the Madden–Julian oscillation and convectively-coupled Rossby waves. *Climate Dynamics*, 46(7), 2155–2178. <https://doi.org/10.1007/s00382-015-2695-x>
- Ren, P., Kim, D., Ahn, M.-S., Kang, D., & Ren, H.-L. (2021). Intercomparison of MJO column moist static energy and water vapor budget among six modern reanalysis products. *Journal of Climate*, 34(8), 2977–3001. <https://doi.org/10.1175/JCLI-D-20-0653.1>
- Ricciardulli, L., & Sardeshmukh, P. D. (2002). Local time- and space scales of organized tropical deep convection. *Journal of Climate*, 15(19), 2775–2790. [https://doi.org/10.1175/1520-0442\(2002\)015<2775:ltasso>2.0.co;2](https://doi.org/10.1175/1520-0442(2002)015<2775:ltasso>2.0.co;2)
- Seiki, A., & Takayabu, Y. N. (2007). Westerly wind bursts and their relationship with intraseasonal variations and ENSO. Part II: Energetics over the western and central Pacific. *Monthly Weather Review*, 135(10), 3346–3361. <https://doi.org/10.1175/MWR3503.1>
- Sobel, A., & Maloney, E. (2013). Moisture modes and the eastward propagation of the MJO. *Journal of the Atmospheric Sciences*, 70(1), 187–192. <https://doi.org/10.1175/JAS-D-12-0189.1>
- Takayabu, Y. N., & Nitta, T. (1993). 3–5 day-period disturbances coupled with convection over the tropical Pacific Ocean. *Journal of the Meteorological Society of Japan*, 71(2), 221–246. https://doi.org/10.2151/jmsj1965.71.2_221
- Tulich, S. N., & Kiladis, G. N. (2021). On the regionality of moist Kelvin waves and the MJO: The critical role of the background zonal flow. *Journal of Advances in Modeling Earth Systems*, 13(9), e2021MS002528. <https://doi.org/10.1029/2021MS002528>
- Wang, L., Li, T., & Chen, L. (2019). Modulation of the Madden–Julian oscillation on the energetics of wintertime synoptic-scale disturbances. *Climate Dynamics*, 52(7), 4861–4871. <https://doi.org/10.1007/s00382-018-4447-1>
- Wang, S., & Sobel, A. H. (2022). A unified moisture mode theory for the Madden–Julian oscillation and the Boreal summer intraseasonal oscillation. *Journal of Climate*, 35(4), 1267–1291. <https://doi.org/10.1175/JCLI-D-21-0361.1>
- Weidman, S., Kleiner, N., & Kuang, Z. (2022). A rotation procedure to improve seasonally varying empirical orthogonal function bases for MJO indices. *Geophysical Research Letters*, 49(15), e2022GL099998. <https://doi.org/10.1029/2022GL099998>
- Wheeler, M., & Kiladis, G. N. (1999). Convectively coupled equatorial waves: Analysis of clouds and temperature in the wavenumber-frequency domain. *Journal of the Atmospheric Sciences*, 56(3), 374–399. [https://doi.org/10.1175/1520-0469\(1999\)056<0374:ccwao>2.0.co;2](https://doi.org/10.1175/1520-0469(1999)056<0374:ccwao>2.0.co;2)
- Wheeler, M. C., & Hendon, H. H. (2004). An all-season real-time multivariate MJO index: Development of an index for monitoring and prediction. *Monthly Weather Review*, 132(8), 1917–1932. [https://doi.org/10.1175/1520-0493\(2004\)132<1917:AARMMI>2.0.CO;2](https://doi.org/10.1175/1520-0493(2004)132<1917:AARMMI>2.0.CO;2)
- Wolding, B. O., Maloney, E. D., & Branson, M. (2016). Vertically resolved weak temperature gradient analysis of the Madden-Julian oscillation in SP-CESM. *Journal of Advances in Modeling Earth Systems*, 8(4), 1586–1619. <https://doi.org/10.1002/2016MS000724>
- Yano, J.-i., Blender, R., Zhang, C., & Fraedrich, K. (2004). 1/f noise and pulse-like events in the tropical atmospheric surface variabilities. *Quarterly Journal of the Royal Meteorological Society*, 130(600), 1697–1721. <https://doi.org/10.1256/qj.03.42>
- Zhang, C., & Dong, M. (2004). Seasonality in the Madden–Julian oscillation. *Journal of Climate*, 17(16), 3169–3180. [https://doi.org/10.1175/1520-0442\(2004\)017<3169:SITMO>2.0.CO;2](https://doi.org/10.1175/1520-0442(2004)017<3169:SITMO>2.0.CO;2)